

## Intermittent turbulence and turbulent structures in a linear magnetized plasma

T. A. Carter<sup>a)</sup>

*Department of Physics and Astronomy and Center for Multiscale Plasma Dynamics,  
University of California, Los Angeles, California 90095-1547*

(Received 9 September 2005; accepted 30 November 2005; published online 10 January 2006)

Strongly intermittent turbulence is observed in the shadow of a limiter in the large plasma device at UCLA [W. Gekelman *et al.*, *Rev. Sci. Instrum.* **62**, 2875 (1991)]. The amplitude probability distribution function of the turbulence is strongly skewed, with density depletion events (or “holes”) dominant in the high-density region and density-enhancement events (or “blobs”) dominant in the low-density region. Two-dimensional cross-conditional averaging shows that the blobs are detached, outward-propagating filamentary structures with a clear dipolar potential, while the holes appear to be part of a more extended turbulent structure. A statistical study of the blobs reveals a typical size of ten times the ion sound gyroradius and a typical velocity of one-tenth the sound speed.

© 2006 American Institute of Physics. [DOI: [10.1063/1.2158929](https://doi.org/10.1063/1.2158929)]

Turbulence which is intermittent, meaning patchy in space or bursty in time, is often observed in both neutral fluids<sup>1</sup> and plasmas.<sup>2</sup> A signature of intermittency in turbulent measurements is a non-Gaussian amplitude probability distribution function (PDF), e.g., with tails caused by a greater frequency of large-amplitude events. Intermittent turbulence is ubiquitous in the edge of magnetic confinement laboratory plasmas including tokamaks,<sup>3</sup> stellarators,<sup>4</sup> and linear devices.<sup>5</sup> The intermittency in these environments is generally attributed to the creation and propagation of filamentary (magnetic-field aligned) structures.<sup>6,7</sup> Large-amplitude events in Langmuir probe,<sup>8</sup> beam-emission spectroscopy,<sup>9</sup> and gas puff imaging measurements<sup>10</sup> are therefore due to the passage of high-density structures through the low-density edge region. The outward propagation of these structures results in significant particle transport in the edge of magnetic confinement devices such as tokamaks.<sup>11</sup> In addition, recently a correlation has been found between increased intermittency in the scrape-off layer (SOL) and the density limit in tokamaks, leading some to suggest that catastrophic transport enhancements associated with intermittent turbulence may be responsible for this disruptive limit.<sup>12</sup>

Several mechanisms have been proposed for the generation of these structures including solitary drift wave vortices,<sup>13,14</sup> propagating avalanche-like events in the plasma core,<sup>15,16</sup> zonal-flow-driven generation,<sup>17</sup> and interchange-driven production.<sup>18</sup> Once the structures are produced and ejected into the low-density region, their continued cross-field propagation has been attributed to  $E \times B$  velocity due to polarization by drift charging.<sup>7,19</sup> In tokamaks, the drift charging is attributed to interchange forces associated with magnetic-field gradients and curvature.<sup>7</sup> In linear devices, rotation<sup>2</sup> is usually invoked as an interchange force.

In this Letter, a detailed study of turbulent structures associated with intermittent turbulence in a linear magne-

tized plasma with a steep density gradient is presented. In this study, a clear observation of both density enhancements (or “blobs”) and density depletions (or “holes”) is made. The production of blob and hole structures is consistent with an interchange-like process. However, the experiments occur in a plasma with straight, uniform magnetic field and without significant rotation due to the straight, vertical edge created by the limiter. The typical interchange forces are therefore not available, yet the resulting intermittency is very similar to that observed in tokamaks. It has been proposed that a frictional force due to neutral flows may serve as an interchange force in cases where rotation or curvature are not present,<sup>20</sup> and this theory may explain the observations. Two-dimensional measurements of cross-field structure show that blobs are isolated structures with a dipolar potential, while the holes are instead part of a more extended structure. A statistical study of the properties of the blobs has been performed, showing that the size of the structures scales like the ion sound gyroradius ( $\delta \sim 10\rho_s$ ) and that the velocity of the objects (outward, into the limiter shadow) scales with the sound speed ( $v \sim C_s/10$ ).

The experiments were performed in the upgraded large plasma device (LAPD), which is part of the Basic Plasma Science Facility<sup>21</sup> (BaPSF) at UCLA. LAPD is an 18-m-long, 1-m-diameter cylindrical vacuum chamber surrounded by 90 magnetic-field coils. Pulsed plasmas ( $\sim 10$  ms in duration) are created at a repetition rate of 1 Hz using a barium oxide coated cathode source. Typical plasma parameters are  $n_e \sim 1 \times 10^{12}$  cm<sup>-3</sup>,  $T_e \sim 5$  eV,  $T_i \sim 1$  eV, and  $B < 2$  kG. The working gases used in these experiments were helium and neon. The length of the LAPD plasma column can be changed by closing a hinged, electrically floating aluminum plate located 10 m from the cathode. In the experiments reported here, this plate is partially closed and used to limit the plasma column as shown in Fig. 1(a). With the plate partially closed, there is no parallel (to the magnetic field) source of plasma for the region behind the plate and any observed plasma density must come from cross-field trans-

<sup>a)</sup>Electronic mail: [tcarter@physics.ucla.edu](mailto:tcarter@physics.ucla.edu)

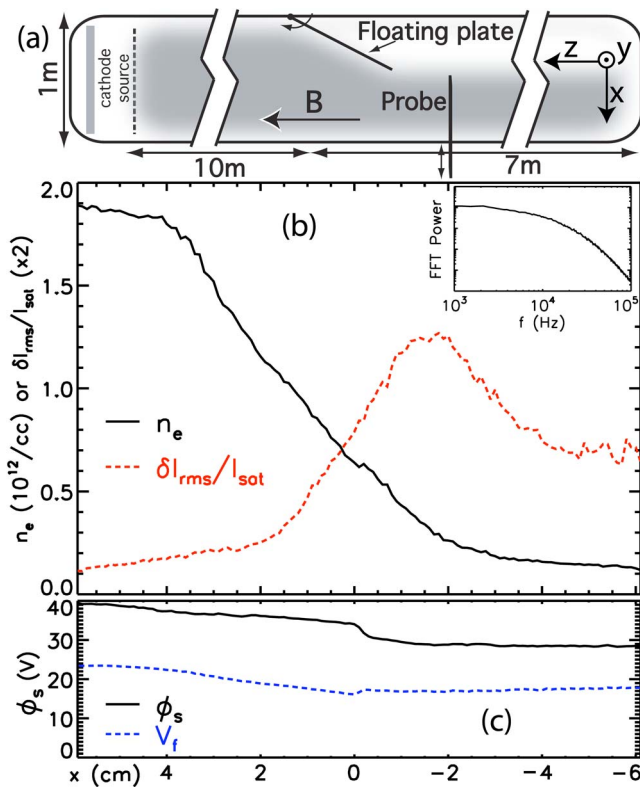


FIG. 1. (Color online). (a) A schematic of the LAPD showing the experimental geometry. (b) Spatial profile of density and fluctuations behind the limiter ( $x=0$  at the limiter edge) along with an average fluctuation power spectrum (log-log). (c) Spatial profile of space potential and floating potential as measured using a triple probe.

port. Measurements were performed using radially insertable Langmuir probes [as shown in Fig. 1(a)]. Triple Langmuir probes with 2-mm-long, 0.76-mm-diameter cylindrical tungsten tips spaced 3 mm apart were used to measure density, electron temperature, and floating potential, and to perform two-dimensional cross-conditional averaging measurements. A linear array of six single Langmuir probes (1.5-mm-diameter flush-mounted tantalum tips spaced 5 mm apart, aligned with their surface normals along the magnetic field) was also used to study the propagation of structures.

For these experiments, the floating-plate limiter was closed so that nearly half of the plasma column is blocked, and a half-cylindrical plasma is observed downstream from the limiter. Steep gradients in plasma density are observed behind the limiter, along with very large amplitude ( $\delta n/n \sim 1$ ) fluctuations. Figure 1(b) shows a measurement of the radial profile of plasma density ( $n_e$ ) and normalized root-mean-square (rms) ion saturation current ( $I_{sat}$ ) fluctuation amplitude ( $\delta I_{rms}/I_{sat}$ ) 0.5 m downstream from the limiter (He discharge, 1.5 kG field) along with an average fast Fourier transform (FFT) power spectrum of the fluctuations. The observed density gradient is very steep with a scale length of the order of a few centimeters (the ion sound radius,  $\rho_s \sim 0.3$  cm, and the ion gyroradius,  $\rho_i \sim 0.15$  cm). In the limiter shadow, the density profile is flat, similar to the profiles observed in the scrape-off layer of tokamaks.<sup>9</sup> The density behind the limiter is a significant fraction of the core density, indicative of substantial cross-field particle transport.

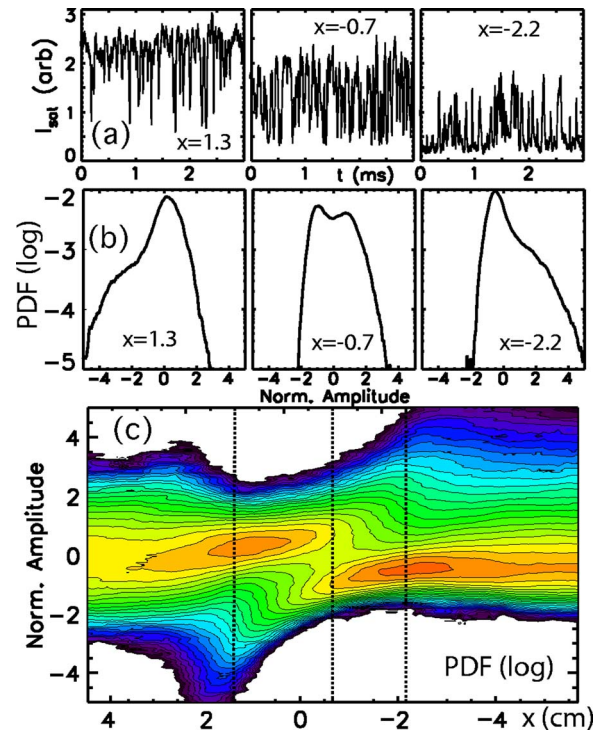


FIG. 2. (Color online). (a) Example raw  $I_{sat}$  signals at three spatial locations. (b) Amplitude PDF at the same three locations. (c) Contour plot of the amplitude PDF vs position.

The FFT power spectrum of the fluctuations is broadband and free from coherent modes. Figure 1(c) shows the profile of space potential (derived from floating potential, also shown) in the plasma. While there is a strong feature in the potential profile near the location of the limiter, indicating a sheared  $E \times B$  flow, there is little or no flow in the region behind the limiter. It is important to note that the limiter has a straight vertical edge. Thus, while there are vertical flows localized to the limiter edge region, there are no rotation and associated centrifugal force.

Figure 2(a) shows example  $I_{sat}$  signals measured at three spatial locations ( $x=1.3, -0.7, -2.2$  cm, where  $x=0$  cm is the edge of the limiter). On the core side of the gradient region ( $x=1.3$  cm), the signal is dominated by downward-going events, while on the low-density side of the gradient region ( $x=-2.2$  cm) the signal is dominated by upward-going events. The upward-going events in the low-density region are density enhancements or blobs, similar to those observed in the edge of many magnetic confinement devices.<sup>2</sup> The downward-going events are identified as density depletions or holes, which are not typically observed in other devices, but have been reported to be seen in measurements on the DIII-D tokamak.<sup>9</sup> Generation of holes has been observed in simulations<sup>22</sup> and inward propagation of holes has been suggested as a mechanism for impurity transport in tokamaks.<sup>23</sup> Although the raw signals clearly show the intermittency in the fluctuations, a more quantitative measurement of the intermittency can be derived from the fluctuation amplitude PDF. The amplitude PDF has been computed as a function of the amplitude normalized to the rms fluctuation level and is shown for  $x=1.3, -0.7$ , and  $-2.2$  cm in Fig. 2(b). The exist-

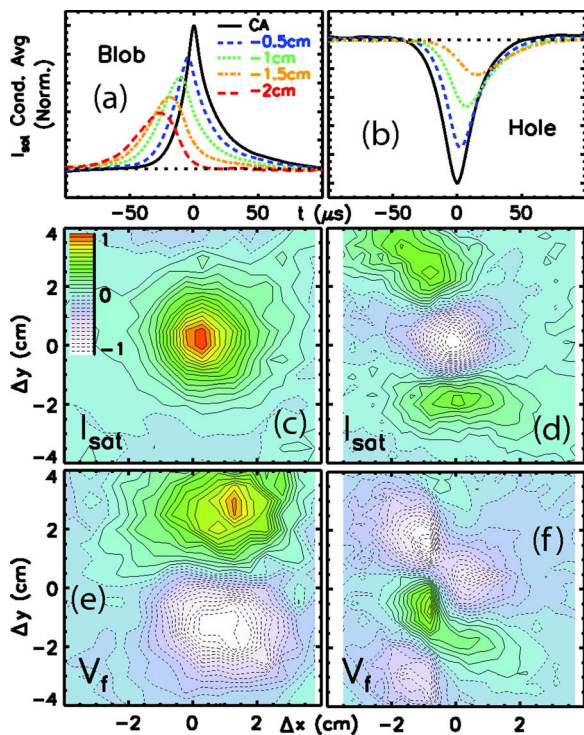


FIG. 3. (Color online). Cross-conditional average of  $I_{\text{sat}}$  on the linear probe array for (a) blob and (b) hole events showing apparent propagation of blobs out of the plasma and holes back into the plasma. Two-dimensional cross-conditional averages of blob [(c)  $I_{\text{sat}}$  and (e)  $V_f$ ] and hole [(d)  $I_{\text{sat}}$  and (f)  $V_f$ ]. All 2D conditional averages are normalized to the maximum of the absolute value of the average, and the color bar in (c) applies to all images.

tence of holes and blobs produces tails in the PDF at negative and positive normalized amplitudes, respectively. The PDF at the location of peak fluctuation amplitude ( $x = -0.7$  cm) is more symmetric, although still distinctly non-Gaussian. The amplitude PDF as a function of position is shown as a contour plot in Fig. 2(c). From this figure it is evident that the holes are observed only in a narrow region of space on the high-density side of the gradient (where the negative tail is present,  $2.8 \geq x \geq 0$ ). However, the blobs are observed everywhere to the right of the density-gradient region ( $x \leq -0.5$ ), as shown by the presence of a tail in the PDF at positive amplitude. For  $x \leq -3$  cm, the PDF is blob dominated and nearly independent of position, suggesting that the blob structures are long-lived as they propagate into the shadow of the limiter (intermittent signals have been observed up to 20 cm beyond the limiter edge). It should be noted that the PDF displayed in Fig. 2(c) exhibits trends which are very similar to those observed using beam-emission spectroscopy in the DIII-D tokamak (see Fig. 3 of Ref. 9). The nature of the intermittency and turbulent structures in these experiments is therefore quite similar to that observed in toroidal confinement devices, even in the absence of magnetic curvature or rotation.

Figure 3(a) shows the conditional average<sup>24</sup> of many ( $N = 16\,059$ ) blob events using  $I_{\text{sat}}$  signals from one tip on the linear Langmuir array (solid black line marked “CA”). The amplitude threshold for triggering event selection in this case was set to twice the root-mean-square fluctuation amplitude. The conditional average blob event is asymmetric in time,

with a fast rise and slow decay. This time asymmetry is consistent with observations in the edge of many other magnetic confinement devices<sup>2</sup> and with simulations.<sup>23</sup> Along with the conditional average, Fig. 3(a) shows the cross-conditional average blob event as measured by other tips in the Langmuir array (separations shown are in the  $-\hat{x}$  direction). The rightmost tip (farthest away from the gradient region in the blob case) is used for event triggering. The average blob appears to travel across the probe array out into the low-density region with a speed of  $\sim 942$  m/s, which is  $\sim C_s/10$ . Figure 3(b) shows the same conditional and cross-conditional averaging for hole events. The average hole decays quickly in space, but appears to propagate back into the core plasma. The interpretation of the Langmuir array conditional averages as being caused by propagation of structures in and out of the core plasma cannot be conclusive without knowledge of the two-dimensional structure of the objects. For example, the observations could also be explained by the vertical ( $\hat{y}$ ) propagation of structures which are tilted in the  $xy$  plane.

In order to conclusively determine the structure and direction of propagation of the holes and blobs, two-dimensional cross-conditional averaging was performed using two triple Langmuir probes separated along the magnetic field by 60 cm. The first probe, which was the reference or trigger probe, was left fixed in space while the second probe was moved to 441 positions in a  $10 \times 10$  cm<sup>2</sup> cross-field ( $xy$ ) plane centered on the position of the reference probe. Figures 3(c) and 3(e) show the 2D cross-conditional average of  $I_{\text{sat}}$  and  $V_f$ , respectively, for blob events (the fixed probe was located at  $x = -3$  cm). The blob is clearly an isolated, detached structure, with similar extent in the two cross-field directions. The  $V_f$  measurement clearly shows a dipole structure of the potential associated with the blob (the peak potential value is  $\sim 1.3$  V, while the minimum value is  $\sim -1.5$  V, here  $T_e \sim 5$  eV). The potential structure is consistent with  $E \times B$  propagation almost entirely in the  $-\hat{x}$  direction with an average speed of  $\sim 985$  m/s. This value is comparable to the speed measured by the linear probe array. Because the blob velocity is dominantly in the  $-\hat{x}$  direction, the decay of the cross-conditional average in Fig. 3(a) can be attributed to a finite spread in the blob velocity. Figures 3(d) and 3(f) show 2D cross-conditional averages for hole events (fixed probe at  $x = 1.5$  cm). The hole does not appear to be an isolated structure, but is instead associated with a turbulent structure that is extended in the vertical ( $\hat{y}$ ) direction. The potential structure does show a tendency for  $E \times B$  propagation back into the core plasma, consistent with the linear array measurements.

Figure 4(a) shows the measured dependence of the time width of blob events versus magnetic field. The inset figure shows the conditional average  $I_{\text{sat}}$  signal for a blob event for three field values. As the field is decreased, the time width of the event increases. The main figure shows the PDF of the time width [full width at half maximum (FWHM)] of blob events for the same three magnetic-field values. To calculate the PDF of the blob time width, events are selected from the  $I_{\text{sat}}$  signals and the time width ( $\Delta t_{\text{FWHM}}$ ) of each individual event is measured. As the magnetic field is decreased, the

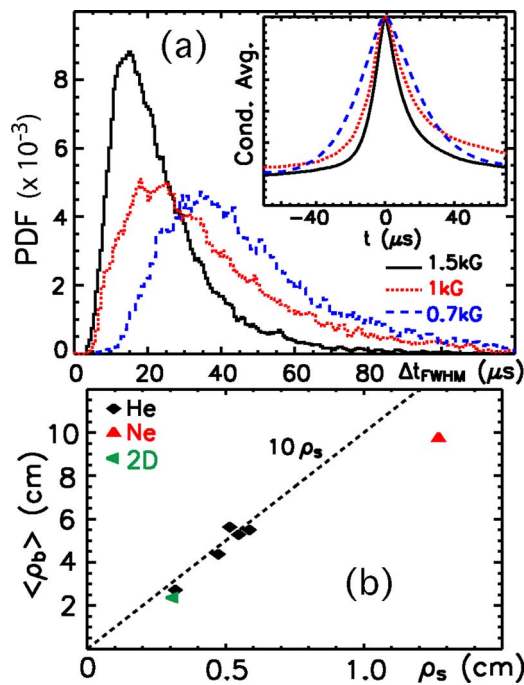


FIG. 4. (Color online). (a) PDF of blob event time width for three values of the magnetic field. The insets are conditional average blob events for the three magnetic-field values. (b) Mean blob size for several conditions in He and Ne compared with the ion sound gyroradius.

peak of the PDF shifts to a larger time width and also the width of the PDF increases. The width in time of the blob event can be translated to a blob size using the blob velocity as measured by the linear probe array. Figure 4(b) shows the average blob size ( $\langle \rho_b \rangle$ ) compared with the ion sound gyroradius ( $\rho_s$ ) for blob events measured in several different magnetic-field values in helium and one condition using neon as the working gas. In addition, the average size obtained from the 1.5 kG 2D cross-conditional average [Fig. 3(c)] is shown. The average blob size scales with the ion sound gyroradius and is approximately ten times this scale. The observation of a gyroradius scaling is consistent with recent theory,<sup>25</sup> which attributes the scaling to blob stability. It should also be noted that the average blob size is also comparable to the density-gradient scale length.

In summary, both blobs and holes are observed to be associated with strongly intermittent turbulence in the shadow of a limiter in LAPD. The blobs are nearly cylindrical filamentary structures which have a dipolar potential, resulting in  $E \times B$  propagation into the low-density limiter shadow. A statistical study of the blobs has been performed, showing that the average speed of the structures is  $\sim C_s/10$  and that the average blob size is  $\sim 10\rho_s$ . The holes do not appear to be detached, propagating objects, but are instead part of a more extended turbulent structure, a finding which might also apply to observations of holes in tokamaks. These

observations are made in an experiment free from traditional interchange forces, yet are very similar to measurements in the edge of toroidal confinement devices. The formation of these turbulent structures and their polarization may be linked to the instabilities associated with sheared flow in the gradient region. The dipolar potential and propagation of blobs may also be explained by drift charging arising from a newly proposed force due to neutral flows. An initial calculation using this theory and LAPD parameters results in a blob velocity which agrees with the experimental observation.<sup>20</sup> The role of sheared flows and neutrals will be explored in more detail in future research.

Discussions with G. Antar, S. Krasheninnikov, R. Moyer, A. Pigarov, and D. Rudakov are gratefully acknowledged.

The experiments reported in the paper were performed using the UCLA Basic Plasma Science Facility, which is funded by NSF and DOE. This work was supported by a DOE Fusion Energy Sciences postdoctoral fellowship and by DOE Grant No. DE-FG02-02ER54688.

- <sup>1</sup>U. Frisch, *Turbulence* (Cambridge University Press, Cambridge, UK, 1995), p. 120ff.
- <sup>2</sup>G. Y. Antar, G. Counsell, Y. Yu, B. Labombard, and P. Devynck, *Phys. Plasmas* **10**, 419 (2003).
- <sup>3</sup>J. Boedo, D. Rudakov, R. Moyer *et al.*, *Phys. Plasmas* **8**, 4826 (2001).
- <sup>4</sup>R. Sanchez, B. van Milligen, D. Newman, and B. Carreras, *Phys. Rev. Lett.* **90**, 185005 (2003).
- <sup>5</sup>G. Y. Antar, S. I. Krasheninnikov, P. Devynck, R. P. Doerner, E. M. Hollman, J. A. Boedo, S. C. Luckhardt, and R. W. Conn, *Phys. Rev. Lett.* **87**, 065001 (2001).
- <sup>6</sup>S. Zweben, *Phys. Fluids* **28**, 974 (1985).
- <sup>7</sup>S. Krasheninnikov, *Phys. Lett. A* **283**, 368 (2001).
- <sup>8</sup>D. Rudakov, J. Boedo, R. Moyer *et al.*, *Plasma Phys. Controlled Fusion* **44**, 717 (2002).
- <sup>9</sup>J. Boedo, D. Rudakov, R. Colchin *et al.*, *Phys. Plasmas* **10**, 1670 (2003).
- <sup>10</sup>S. Zweben, D. Stotler, J. Terry *et al.*, *Phys. Plasmas* **9**, 1981 (2002).
- <sup>11</sup>D. D'Ippolito, J. Myra, and S. Krasheninnikov, *Phys. Plasmas* **9**, 222 (2002).
- <sup>12</sup>M. Greenwald, *Plasma Phys. Controlled Fusion* **44**, R27 (2002).
- <sup>13</sup>A. Hassam and R. Kulsrud, *Phys. Fluids* **22**, 2097 (1979).
- <sup>14</sup>W. Horton, *Phys. Fluids B* **1**, 524 (1989).
- <sup>15</sup>P. Diamond and T. Hahm, *Phys. Plasmas* **2**, 3640 (1995).
- <sup>16</sup>D. Newman, B. Carreras, P. Diamond, and T. Hahm, *Phys. Plasmas* **3**, 1858 (1996).
- <sup>17</sup>A. Smolyakov, P. Diamond, and M. Malkov, *Phys. Rev. Lett.* **84**, 491 (2000).
- <sup>18</sup>O. Garcia, V. Naulin, A. Nielsen, and J. Rasmussen, *Phys. Rev. Lett.* **92**, 165003 (2004).
- <sup>19</sup>F. Chen, *Sci. Am.* **217**, 76 (1967).
- <sup>20</sup>S. Krasheninnikov and A. Smolyakov, *Phys. Plasmas* **10**, 3020 (2003).
- <sup>21</sup>W. Gekelman, H. Pfister, Z. Lucky, J. Bamber, D. Leneman, and J. Maggs, *Rev. Sci. Instrum.* **62**, 2875 (1991).
- <sup>22</sup>D. A. Russell, D. A. D'Ippolito, J. R. Myra, W. M. Nevins, and X. Q. Xu, *Phys. Rev. Lett.* **93**, 265001 (2004).
- <sup>23</sup>D. A. D'Ippolito, J. R. Myra, S. I. Krasheninnikov, G. Q. Yu, and A. Y. Pigarov, *Contrib. Plasma Phys.* **44**, 205 (2004).
- <sup>24</sup>A. V. Filippas, R. D. Bengston, G. X. Li, M. Meier, C. P. Ritz, and E. J. Powers, *Phys. Plasmas* **2**, 839 (1995).
- <sup>25</sup>D. D'Ippolito, J. Myra, D. Russell, and G. Yu, *Phys. Plasmas* **11**, 4603 (2004).